Efficient Deployment of UAV-powered Sensors for Optimal Coverage and Connectivity

Oktay Cetinkaya Geoff V. Merrett
Centre for IoT and Pervasive Systems
School of Electronics and Computer Science
University of Southampton, Southampton SO17 1BJ, UK
{oc1y18, gvm}@ecs.soton.ac.uk

***Abstract*—The Internet of Things (IoT) digitizes the physical world with wireless devices sensing their surroundings and delivering periodic notifications of parameters they are monitoring. However, this operation is bound by finite-capacity batteries, in which replenishment is practically infeasible due to the envisioned size of the IoT networks. By also considering the autonomous and self-sufficient service vision of the IoT paradigm, the need for novel approaches overcoming the energy constraints is evident. Here, unmanned aerial vehicles (UAVs) come into prominence. The UAVs can remotely energize wireless devices, via wireless power transfer (WPT), and thus guarantee reliable sensing coverage as well as longevity in the IoT domain. However, this can be only achieved by the precise alignment of both UAVs and wireless devices. Thus, this paper presents an efficient deployment strategy based on the *circle packing problem*, in which a lower-bound for the required number of wireless devices achieving optimal coverage is derived. The analysis, based on empirical measurements, reveals the design considerations for an energy harvesting (EH)-aided UAV scenario with regard to Federal Communications Commission (FCC) regulations, power consumption of wireless devices, and reporting frequency requirements of the IoT applications. Our results elaborate on a number of trade-offs, based on UAV, device, and medium characteristics, and provide realistic guidelines, achieving optimal coverage while meeting application requirements.**

***Index Terms*—Wireless Power Transfer, Unmanned Aerial Vehicles, Internet of Things, Network Coverage, Deployment.**

I. Introduction

The recent proliferation of unmanned aerial vehicles (UAVs) [1] draws considerable attention to the alleviation of energy constraints in the Internet of Things (IoT) [2]. The use of UAVs in (remote) powering of wireless devices, i.e. sensors, has a great potential to achieve perpetual and autonomous monitoring, especially for hard-to-reach mediums lacking in infrastructure and human support. The UAVs can enable rapid, on-demand, and high efficient power delivery thanks to the line-of-sight (LoS) air-to-ground links. This can greatly enhance service quality, i.e. reporting frequency or sensing coverage provided by energy-constrained wireless devices. The UAVs can also operate as (mobile) access points (APs), providing connectivity throughout the IoT networks. Furthermore, if the energy required for the UAV operation, including wireless power transfer (WPT) [3] to the devices, is provided by recharging stations that are capable of energy harvesting (EH) [4], the vision of *energy-neutral wireless-powered networks* [5] may become achievable.

The idea of WPT with EH-aided UAVs, however, is not entirely new [6]. There are also a plethora of studies focusing on different aspects of UAV operation to address the ongoing challenges [7], such as resource management, flight path and energy optimization, and interference minimization. Among them, efficient deployment of both UAVs and wireless devices come to the forefront [8]–[10], as it not only impacts the system performance but also intensifies other problems. However, the existing works on this topic partially or fully disregard some aspects that immensely affect the operation, which inevitably causes a discrepancy between the theory and practice. Thus, to tackle this problem and provide a more realistic analysis, this paper conducts an investigation on deployment/coverage by considering: 1) a limited source of power for WPT, i.e. an EH-aided UAV; 2) effective isotropic radiated power (EIRP) limitations enforced by the regulatory organizations, e.g. Federal Communications Commission (FCC); 3) power consumption of wireless devices; and 4) reporting frequency requirements of the IoT applications.

This work aims to convey a high-level discussion on the efficient deployment of network components, i.e. the UAV and wireless devices, to achieve optimum coverage over an event area of interest. With this agenda, we first derive the sensing range of wireless devices. Then, by using the *circle packing problem* (CPP) [11], we formulate a well-planned deployment strategy avoiding overlaps and oversteps, and thus enable efficient and interference-free operations. The analysis, based on empirical measurements, reveals the non-trivial relationships between the UAV attributes (e.g. altitude, directivity, energy budget, output power, transmission duration and frequency); device characteristics (e.g. quantity, sensing model, power consumption and conversion efficiency); medium specifications (e.g. path loss, event area); and application requirements (e.g. reporting frequency, throughput). In the end, this paper provides a lower-bound for the required number of wireless devices ensuring optimal coverage, which can be practically obtained by the careful selection of design parameters in a UAV-powered energy-neutral application scenario.

The remainder of this paper is organized as follows. We first introduce the system model in Sec. II, where the effect of directivity, adopted WPT model, rectenna operation, the FCC regulations, and the fundamental assumptions are explained. Accordingly, the (maximum) sensing range of wireless devices

is derived. Sec. III outlines the conventional deployment models and formulates an efficient deployment strategy based on CPP, providing a lower-bound for the required number of wireless devices (by using the sensing range devised). This is followed by the numerical evaluation of the proposed model in Sec. IV to reveal the design guidelines needed to be followed to achieve optimal coverage while meeting application requirements. Finally, Sec. V concludes the paper.

II. System Model

The network scenario shown in Fig. 1 is envisioned in a hierarchical order employing star topology between one UAV and N wireless-powered devices (w-pDs). The UAV retrieves energy from an EH recharging station, flies to the event area, and conveys the borrowed energy in a "point-to-multipoint" fashion to the identical w-pDs deployed on the ground plane. During the WPT stage, the UAV do not move in the 3D space. The w-pDs operate as battery-less sensors, i.e. they probe their vicinity for an application-defined parameter and notify higher-level authorities via an IP-enabled remote AP, which can be the UAV in some cases. Since the w-pDs are powered by the UAV, they operate as long as they intercept enough power.

The UAV performs WPT with a directional antenna having a pencil-beam-like radiation pattern. For such an antenna, i.e. with one major lobe and very negligible minor lobs of the beam, the gain G_T can be approximated by

$$G_T = \begin{cases} \approx \dfrac{30000}{\theta_B^2}, & \frac{-\theta_B}{2} \leq \varphi \leq \frac{\theta_B}{2}, \quad \text{(major lobe)} \\ g(\varphi), & \text{otherwise}, \quad \text{(minor lobes)} \end{cases} \tag{1}$$

where φ is the sector angle, θ_B is the directional antenna half-power beamwidth (HPBW) -both in degrees, $\approx 30000/\theta_B^2$ is the maximum gain, and $g(\varphi)$ is the gain outside of the major lobe (including minor lobes), which can be neglected [12]. Note that (1) is for a symmetrical radiation pattern, in which the HPBWs in each plane are equal to each other, i.e. $\theta_{1d} = \theta_{2d}$.

For the scenario depicted in Fig. 1, the radiation of UAV resembles a cone with slant height R_{RF}, apex angle θ_B, base radius r_u, and height h. Thus, from the projection of this radiation, the geographical (*or* event) area to be powered is $\Delta_{UAV} = \pi r_u^2 = \pi R_{RF}^2 sin^2 \frac{\theta_B}{2}$. As seen, θ_B alters not only G_T given by (1) but also Δ_{UAV}. Any increment in Δ_{UAV}, by keeping the other parameters constant, accordingly necessitates more than N w-pDs to be deployed. However, the factor that affects N the most is R_{RF}, which is the maximum distance that the UAV can deliver the minimum power required by the w-pDs ($P_{R^{min}}$). Let's consider this power as a function of Euclidean distance between the UAV and w-pDs. Then, $|P_{R^{min}}(r)|$ for the diameter of the base circle will look like the probability density function of a normal distribution with zero mean and very high variance. This is the corollary of directivity, since θ_B is small; thus, $R_{RF} \approx h$. We, therefore, assume that the received power P_R will be equal for each point in the base circle, i.e. the w-pDs will receive the same P_R irrespective of their location.

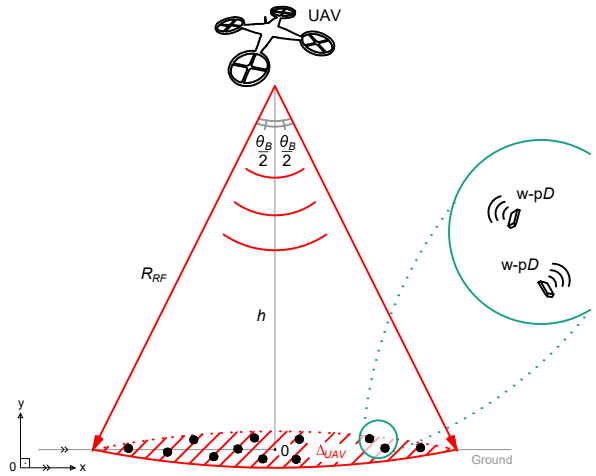

Figure 1: Orientation of network components (cross-sectional view).

Consequently, P_R at distance R_{RF} due to the UAV with transmit power P_T can be given by Friis Transmission Equation [12] as

$$P_R = P_T \frac{G_T G_R \lambda^2}{(4\pi)^2 R_{RF}^{v_1}}, \text{ and } \lambda = \frac{c}{f}, \tag{2}$$

where G_R is the antenna gain of the w-pDs, λ is wavelength, c is the speed of light, f is the carrier frequency of RF waves transmitted by the UAV, and v_1 is the path loss exponent of the air-to-ground channel. This equation refers to the generic RF power transfer model, with no reflected signal between the UAV and w-pDs. It is also assumed that the w-pDs are in LoS of the UAV, and there is no shadowing.

Contrary to expectations, the output power of the UAV in (2), cannot be altered casually; it is bound by the FCC regulations. FCC Part 15.247 rules declare that the maximum P_T fed into the antenna cannot exceed 30dBm (1W) for the ISM bands, and the maximum effective isotropic radiated power (EIRP) is limited to 36dBm (4W) [13]. This indicates that increasing G_T necessitates a proportional decrease in P_T, and vice versa, such that the total RF power radiated by the antenna remains the same, i.e. 4W EIRP. For directional dispersion, on the contrary, there are some exceptions to the maximum EIRP. For example, in the 2.4GHz band, increasing G_T to get an EIRP above 36dBm is allowed (up to 52dBm), where P_T must be reduced by 1dBm for every 3dBi increase of G_T. However, the physical size of the antennas increases with increasing G_T, which is impractical for sensors requiring small form factors. Besides, WPT at high frequencies is not useful as P_R is inversely proportional to the square of the frequency. Thus, at 2.4GHz, a power source increasing its EIRP (with G_T) has to decrease its P_T to comply with the FCC regulations. As the UAV in our case has a fixed energy budget E_H, decreasing P_T allows a longer duration of power transmission t_T, i.e. lengthened coverage lifetime. Although this sounds attractive, the duty cycle of the w-pDs will accordingly be altered, which cannot be tolerated always due to the certain reporting frequency requirements of the IoT applications [14]. Furthermore, since decreasing P_T (increasing f) will accordingly lower P_R, the w-pDs may need to switch

from power-neutral to energy-neutral operation [15], which is not desired for this particular scenario. Thus, these trade-offs must be carefully considered during the system design to maximize the performance metric defined by the application.

It should also be noted that P_R in (2) indicates the power intercepted by the w-pDs (*or* the input power), which has to be converted into usable DC power, P_{har}, by a rectifying antenna (rectenna). Usually, a linear EH function is adopted for this operation, i.e. $P_{har} = \eta P_R$, where η $(0 \leq \eta < 1)$ is the RF-to-DC conversion efficiency of the rectenna. However, this model does not hold in practice due to the non-linearity of diodes, inductors, and capacitors used in the EH circuitry. Empirical results show that η often increases with increasing P_R and remains constant when P_R exceeds the saturation power threshold, P_{sat}, of the harvester [3]. Thus, η is neither a constant nor a linear parameter; it is a function of P_R, where P_R is based on several variables as seen in (2). By also considering the sensitivity of rectenna, i.e. the minimum (threshold) power P_{th} required for its activation, the most accurate EH model can be given by the following piecewise linear function [16]

$$P_{har}(P_R) \triangleq \begin{cases} 0, & P_R \in [0, P_{th}), \\ \eta(P_R) \cdot P_R, & P_R \in [P_{th}, P_{sat}], \\ P_{har}(P_{sat}), & P_R \geq P_{sat}, \end{cases} \tag{3}$$

which is non-decreasing and continuous for all $P_R \in \mathbb{R}$, $P_R \geq 0$. By using curve-fitting tools for any empirical dataset, the function $\eta(\cdot)$ can be simply formulated as a polynomial, which gives a mathematically tractable expression with sufficient precision. In this work, the rectennas are assumed to operate in the ideal region, i.e. $P_R \in [P_{th}, P_{sat}]$ for all w-pDs.

Now, let's suppose that the w-pDs behave as omni-directional radars, where they forward the power delivered by the UAV to their vicinity for the detection of any *thing* of interest at distance r_s. Since the w-pDs are assumed to receive the same P_R and are identical, they will radiate at the same transmit power P'_T, which will result in equal sensing regions for all. Thus, the received, i.e. backscattered, signal strength at a w-pD, which is reflected from the target(s), can be characterized by the well-known radar equation [12] as

$$P_{R^{Rad}} = \overbrace{\underbrace{\frac{P'_T G'_T}{4\pi r_s^{v_2}}}_{\substack{\text{power density} \\ \text{at the target} \\ \text{(due to TX)}}} \times \underbrace{\frac{\sigma}{4\pi r_s^{v_2}}}_{\substack{\text{signal reflected} \\ \text{from the target(s)}}}}^{\substack{\text{backscattered power} \\ \text{density at the RX}}} \times \underbrace{\frac{G'_R c^2}{4\pi f_R^2}}_{\substack{\text{antenna aperture} \\ (A_e) \text{ of the RX}}}, \tag{4}$$

where G'_T and G'_R are respectively the transmitter (TX) and receiver (RX) antenna gain of the w-pD, σ is the radar cross-section of the target(s), and v_2 is the path loss exponent on the ground plane. Here, the w-pDs will use the same antenna for TX and RX, i.e. monostatic radar, and thus $G'_T = G'_R = G_{Rad}$. Furthermore, due to losses and savings for future operations, e.g. processing of the sensed parameters and their transfer to the AP, the w-pDs will only have a portion of P_{har} to forward, i.e. $P'_T = \beta P_{har}(P_R) = \beta \eta(P_R) P_R$, where β is the loss factor.

In (4), if r_s is assumed as the maximum distance that a w-pD can reach, $P_{R^{Rad}}$ turns into the receiver sensitivity, i.e. the minimum power that has to be received to detect a target. For radars, $P_{R^{Rad}}^{min}$ is given by $kT_0BF(S/N)_{min}$, where k is the Boltzmann constant, T_0 is the absolute temperature of the w-pD input, B is the w-pD bandwidth, F is noise factor, and $(S/N)_{min}$ is the minimum signal-to-noise ratio needed to process a signal. The region to be probed by a w-pD will therefore be a small circle with radius $r_s{}^{max}$, i.e. sensing range. By substituting (1), (2), and (3) in (4), and rearranging the resulting equation, $r_s{}^{max}$ can be expressed as

$$r_s{}^{max} = \left(\frac{95.735 \times 10^{-3} \beta \eta(P_R) P_T G_R G_{Rad}^2 \sigma c^4}{f^2 f_R^2 \theta_B^2 R_{RF}^{v_1} k T_0 B F (S/N)_{min}} \right)^{\frac{1}{2v_2}}. \tag{5}$$

It should be noted that sensing range for any sensor can be alternatively given by $r_s = (P'_T/\mu)^{1/\xi}$ [17], instead of the radar assumption, where μ is an application-dependent constant, and ξ is a parameter referring to the power consumption model. In conclusion, (5) -or the above-given equation, can be used to designate relevant design parameters enabling effective sensing coverage in the given deployment scenario.

III. W-PD Deployment: Optimal Coverage

To ensure optimal coverage over the event area Δ_{UAV}, the network must be carefully designed according to the UAV, w-pD, and medium characteristics. Here, the coverage refers to sensing quality of the network, and k-coverage implies that every single point in Δ_{UAV} is sensed by at least k $(0 \leq k \leq N)$ w-pDs. For coverage, two conventional models stand out: random, i.e. no strategy, and grid-type *or* well-planned deployment, as shown in Fig. 2. Regardless of the adopted model, P_{har} given by (3) must be $\geq P_{R^{min}}$ of the w-pDs. This is to reliably sense Δ_{UAV} and deliver the measurements to a remote AP, i.e. guaranteed coverage over the event area and connectivity in the network.

The key factor deriving k-coverage for a random deployment is the sensing range $r_s{}^{max}$ of the w-pDs. This can be simply determined via *stochastic geometry* [18], where k depends on the homogeneous Poisson point process of the w-pD density.

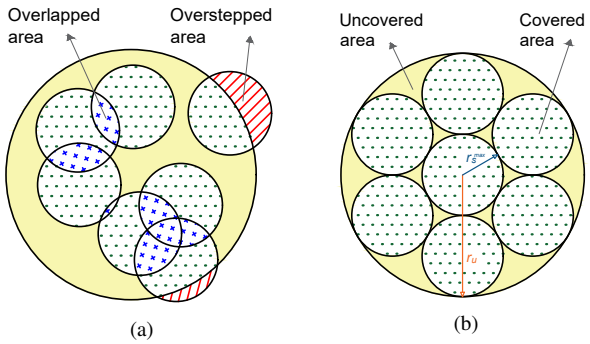

Figure 2: Possible deployment models: (a) no strategy (random); (b) well-planned (grid-type). Small circles represent the sensing regions of the w-pDs, where the big circle is Δ_{UAV}.

Stochastic geometry allows derivation of a tractable expression for k ensuring certain coverage probability, assuming that w-pDs are randomly and uniformly positioned over the event area. However, k, calculated by stochastic geometry is denoted as the worst-case scenario since the sensing regions of w-pDs may overlap, which would necessitate more w-pDs to be deployed for achieving the same coverage rate, D_v. By also considering that radar assumption may not properly work in the case of random positioning due to false alarms, grid-type deployment seems preferable as it may achieve a higher D_v for the same k or the same D_v with less than k w-pDs.

For a *well-planned* deployment, the w-pDs must be positioned in a way such that each point in Δ_{UAV} falls into only one w-pD's sensing range, i.e. no overlaps occur (*constraint* #1). In addition, for the most efficient utilization of the w-pDs, the areas that they cover must stay within Δ_{UAV}, i.e. no oversteps allowed (*constraint* #2). These will potentially allow N to be minimized at the cost of initial deployment. By considering a circular sensing region of $\pi r_{s^{max}}^2$ for each w-pD, the problem can be formulated as

$$\max \quad D_v = \frac{N r_{s^{max}}^2}{R_{RF}^2 sin^2 \frac{\theta_B}{2}}, \tag{6}$$

$$\text{s.t.} \quad (x_i - x_j)^2 + (y_i - y_j)^2 \geq (2 r_{s^{max}})^2, \; i \neq j \in \{1,..,N\}, \tag{7}$$

$$x_i^2 + y_i^2 \leq (R_{RF} sin \frac{\theta_B}{2} - r_{s^{max}})^2, \; x_i, y_i \in \mathbb{R}, \; i \in \{1,..,N\}, \tag{8}$$

$$R_{RF} sin \frac{\theta_B}{2} \geq r_{s^{max}} \geq 0, \tag{9}$$

where x_i and y_i refers to the Cartesian coordinates of w-pD_i on the ground plane (considering Δ_{UAV}'s center as the origin), (7) is *constraint* #1 and (8) is *constraint* #2, explained above. Here, (7) guarantees also that there will be no collision or interference between the w-pDs. In other terms, if the distance between the w-pD and a target is $r_{s^{max}}$, there cannot be any w-pD closer than $r_{s^{max}}$ to that particular target. Finally, (9) is an obvious upper bound for the sensing range.

Solving (6), i.e. maximizing D_v with a minimum N, is not easy due to the above-formulated constraints, the FCC regulations, and a number of variables that depend on UAV attributes. Thus, we model (6) by using the *circle packing problem* (CPP) [11]. In CPP, N circles, which refer to the number of w-pDs, and their corresponding (sensing) areas -for our case, are arranged in a given surface, i.e. Δ_{UAV}, such that the packing density, D_v, is maximized without any overlaps and oversteps. It should be noted that CPP in a given surface is often intractable [8], i.e. it is not likely to constitute a general packing strategy that is optimal for any N. For example, both mirror and square symmetry achieve the same D_v (0.5556) for $N=5$, while pentagonal packing outperforms those two with D_v of 0.6852. Depending on N, new symmetry types, which were not applicable earlier or performed worse, may stand out.

In (6), for a fixed Δ_{UAV}, i.e. constant denominator, $r_{s^{max}}$ decreases for increasing N. D_v, on the other hand, is not strictly increasing, which makes the problem more difficult to solve. In CPP, N is usually given and the main goal is to find the radius of small circles covering a bigger circle (*or* container) for the highest D_v. However, in our case, since the energy budget of the UAV is limited, we can calculate the maximum radius that the circles can have, i.e. $r_{s^{max}}$, which gives the minimum number of N to be deployed. Thus, CPP will provide a lower-bound for N, which is again subject to several variables.

Now, let's define χ as the ratio of the UAV base radius to w-pD sensing range, i.e. $\chi = \frac{R_{RF} sin(\theta_B/2)}{r_{s^{max}}}$, and assume N is the required number of w-pDs to pack the area covered by UAV. In [19], an upper bound for χ is given as

$$\chi \leq \frac{\sqrt{(4q_h - 1)^2 + 16 q_h (N-1)} - 1}{4 q_h} + 1, \tag{10}$$

where q_h denotes the density of hexagonal lattice packing, i.e. $q_h = \frac{\pi}{2\sqrt{3}}$. By using (10) and [20], N can be conjectured as

$$N \geq \left\lceil q_h \chi^2 - (2q_h - \tfrac{1}{2})\chi + \zeta \right\rceil, \; \{\chi \in \mathbb{R} : \chi \geq 1 \,(\text{from}\,(9))\}, \tag{11}$$

where $\zeta = 2$ for $3 \leq \chi < 10$, and $= 1$ otherwise. By using N from (11), the coverage rate can be calculated as $D_v = \frac{N}{\chi^2}$. It should be noted that the maximum D_v that can be achieved by hexagonal lattice packing is ≈ 0.907, i.e. q_h.

IV. Simulation Results and Discussion

For simulations, we consider the UAV-based WPT at 4W EIRP over f of 868MHz (unless otherwise stated) in a suburban area, where the w-pDs have $G_R = G_{rad} =$ 6dBi and $P_{R^{Rad}}^{min}$ of 10^{-9}. The other constant parameters are as follows: $c = 3 \times 10^8$m/s, $f_R = 2.45$GHz, $v_1 = 2.2$ [21], $v_2 = 4.7$ [22], $\sigma = 0.01\text{m}^2$, and $\beta = 0.8$. Furthermore, η is calculated as a function of P_R by using real data outsourced from [23] and [24]. Fig. 3(a) and (b) depict the fitted functions of the used rectenna designs operating at 0.868 and 2.45GHz, respectively.

Fig. 4(a) and (b) show the number of w-pDs, N, and the coverage rate, D_v (corresponds to each N) as a function of altitude, h. Not surprisingly, as the height of UAV increases, more N is needed. This is because the w-pDs receive less P_R and Δ_{UAV} gets larger with increasing h. For a fixed h, lower G_T (*or* higher θ_B) necessitates more N to be deployed, since the power dispersion is performed towards a wider area, i.e. larger Δ_{UAV} to be packed. D_v, on the other hand, is not always increasing due to the constraints explained in the previous section. Fig. 4(c) illustrates the change in N and D_v as well as

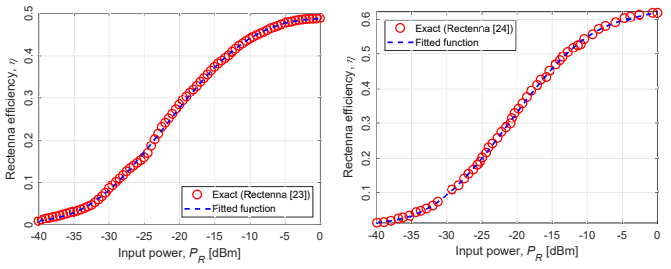

(a) (b)

Figure 3: The rectenna efficiency, η, as a function of input power, P_R: (a) for the rectenna proposed in [23] (@$f_{rect} =$868MHz); (b) for the rectenna proposed in [24] (@$f_{rect} =$2.45GHz).

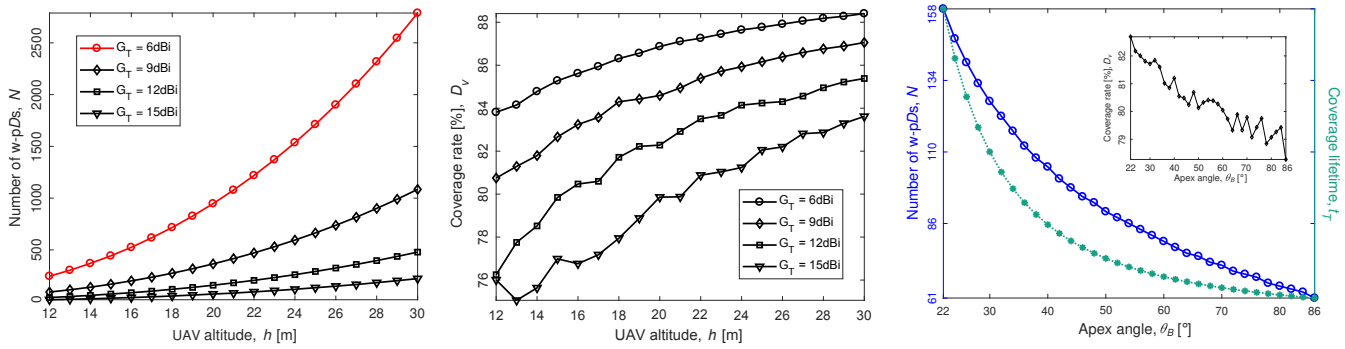

(a) (b) (c)

Figure 4: The number of w-pDs, N, coverage rate, D_v, and coverage lifetime, t_T, for UAV altitude, h, and apex angle, θ_B (4W EIRP @$f=$868MHz): (a) N vs. h; (b) D_v vs. h (for G_T of 6, 9, 12, and 15dBi); (c) N and D_v vs. θ_B and t_T vs. θ_B (for Δ_{UAV} of 140m^2).

coverage lifetime t_T for varying θ_B. Due to the fixed energy budget of the UAV, E_H, the duration of power transmission, t_T, is limited by P_T. In other terms, t_T will decrease proportionally to any increase in P_T, and vice versa, as a corollary of $E_H = P_T \times t_T$, since the UAV is assumed to perform WPT always at the maximum output power allowed by the FCC (4W EIRP). Hence, as seen in Fig. 4(c), increasing θ_B, i.e. decreasing G_T, will allow P_T to be increased as much as possible without violating the maximum EIRP rule, which will accordingly shorten t_T. It should be noted that dynamic change in θ_B (*or* G_T) is not possible in practice. This is just to provide more insights on the characteristics of directional WPT with a limited source of power.

Fig. 5 can be considered as a derivative of Fig. 4(a) and (b), where N and D_v are given as a function of Δ_{UAV}. As seen, (unlike Fig. 4) N is higher for higher G_T at a fixed Δ_{UAV}, since the UAV with higher G_T has to climb up for keeping the Δ_{UAV} constant (due to the narrower θ_B). In practice, some applications requiring coverage over a fixed event area or the medium of interest (e.g. urban areas) may have some restrictions on the lowest h, i.e. the closest altitude approachable. Thus, the UAV has to be equipped with the most suitable antenna to achieve the highest D_v with a minimum N while meeting the application requirements/complying with the specific regulations.

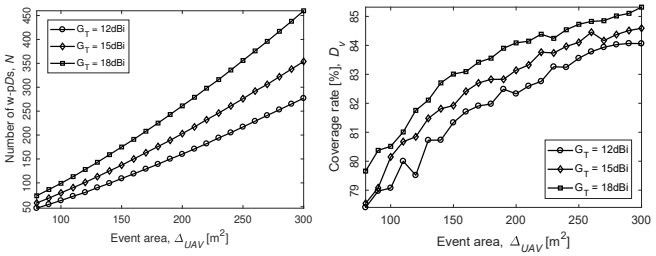

(a) (b)

Figure 5: The number of w-pDs N and coverage rate D_v for the increasing size of event area Δ_{UAV}: (a) N vs. Δ_{UAV}; (b) D_v vs. Δ_{UAV} (for G_T of 12, 15, and 18dBi, 4W EIRP @$f=$868MHz).

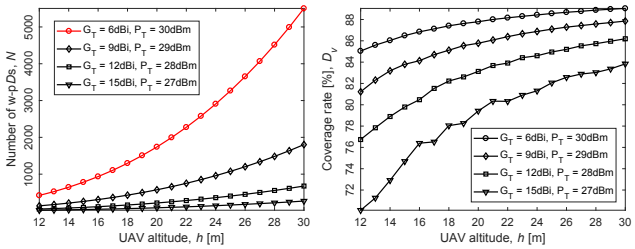

(a) (b)

Figure 6: The effect of increasing EIRP on the number of w-pDs, N, and coverage rate, D_v, for varying UAV altitude, h: (a) N vs. h; (b) D_v vs. h (for EIRP of $\approx$4, 6.31, 10, and 15.85W @$f=$2.45GHz).

Fig. 6 compares the same parameters in Fig. 4(a) and (b) but for an increasing EIRP at f of 2.45GHz. Despite the increase in EIRP (from 4 to 15.85W), the required number of w-pDs, N, has considerably increased since the signal fading is severer at higher f, i.e. $P_R \propto 1/f^2$. Thus, P_R reduces by $\approx$8 times (for the same EIRP) when f changes from 868MHz to 2.45GHz. Note that the red lines in Fig. 4(a) and Fig. 6(a) correspond to the same EIRP (4W or 36dbm, i.e. 6dBi of G_T + 30dBm of P_T). Even for the highest EIRP considered (15.85W), P_R is still half of the value that is achieved at 868MHz with 4W EIRP. Reducing P_R also reduces η, as can be observed from Fig. 3, which adversely affects $r_{s^{max}}$, and thus N. Hence, if the application necessitates the use of 2.45GHz band for the WPT, the UAV should operate on the highest EIRP (considering the antenna size) at the lowest altitude possible. In such a way, the effect of frequency and fading components can be minimized, achieving similar performance to that of the sub-GHz bands. Yet, the increase in the EIRP may affect the duty cycle *or* reporting frequency of the w-pDs since the UAV will need frequent replenishment due to the increased power output, i.e. more trips to the recharging station (duration of which is orders of magnitude longer than t_T). Furthermore, in addition to the lower P_R received by the w-pDs, the throughput at the AP will decrease due to the total time elapsed. These trade-offs point out the need for a more inclusive and complex optimization problem, which is not in the scope of this paper.

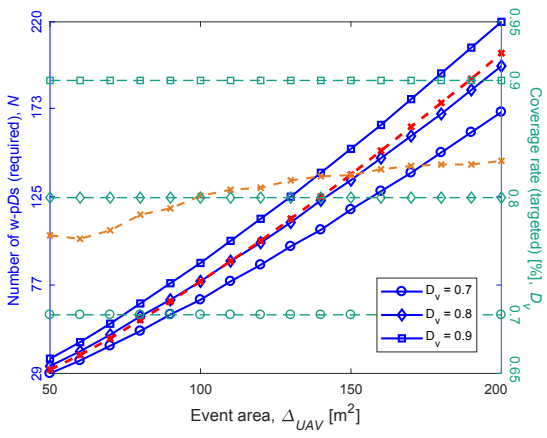

Figure 7: The number of w-pDs required, N, to achieve different target coverage rates, D_v, when increasing size of event area Δ_{UAV} ($\theta_B \approx 30°$, 4W EIRP @$f = 868$MHz). The dashed red line shows N that can be fit in the given Δ_{UAV} (with respect to system parameters), where achievable D_v for that N is shown in orange.

Fig. 7 shows the minimum number of w-pDs required to satisfy a targeted coverage rate over the event area of interest. For any given Δ_{UAV} (from 50 to 200m^2), a D_v of 0.7 can be achieved by a UAV having G_T of 15dBi and transmitting 4W of EIRP at 868MHz. However, for $D_v = 0.8$, Δ_{UAV} must be at least 100m^2. This is a corollary of CPP, i.e. the more w-pDs to be deployed, the higher D_v will be achieved (which occurs only if Δ_{UAV} gets larger or $r_{s^{max}}$ becomes shorter for the same Δ_{UAV}). For the envisioned setting, 0.9 of D_v is not achievable as it needs more than N w-pDs that can fit in the given Δ_{UAV}. Depending on θ_B, P_T, f, and Δ_{UAV}, achievable D_v varies with N. Thus, optimal designation of the relevant design parameters is of utmost importance to meet the requirements (e.g. minimum N, maximum D_v, certain reporting frequency, and highest throughput) set by the applications.

V. Conclusions

This paper investigates the optimal coverage in the IoT networks with a minimum number of w-pDs, which are remotely powered by an energy-limited UAV with a directional antenna. First, the maximum sensing range of the w-pDs was derived as a function of UAV altitude, output power, and directivity. Then, by using the CPP theorem, an efficient deployment strategy avoiding the overlaps and oversteps, and thus providing a lower-bound for the required number of w-pDs was proposed. The analysis revealed the design considerations for maximum coverage with regard to the FCC regulations, realistic rectenna operation, and minimum power and reporting frequency requirements of the w-pDs. Future work will focus on the optimization of the afore-mentioned trade-offs to maximize the throughput in the UAV-powered energy-neutral networks.

VI. Acknowledgment

This work was supported by the UK EPSRC under EP/P010164/1. Simulation data can be found at DOI: 10.5258/SOTON/D1221.

References

[1] S. Hayat, E. Yanmaz, and R. Muzaffar, "Survey on Unmanned Aerial Vehicle Networks for Civil Applications: A Communications Viewpoint," *IEEE Commun. Surv. Tutor.*, vol. 18, no. 4, pp. 2624–2661, FQ 2016.

[2] O. B. Akan *et al.*, "Internet of Hybrid Energy Harvesting Things," *IEEE Internet of Things Journal*, vol. 5, no. 2, pp. 736–746, Apr. 2018.

[3] X. Lu *et al.*, "Wireless Networks With RF Energy Harvesting: A Contemporary Survey," *IEEE Communications Surveys Tutorials*, vol. 17, no. 2, pp. 757–789, Secondquarter 2015.

[4] O. Cetinkaya and O. B. Akan, "Electric-Field Energy Harvesting in Wireless Networks," *IEEE Wireless Communications*, vol. 24, no. 2, pp. 34–41, Apr. 2017.

[5] O. Cetinkaya *et al.*, "Energy-Neutral Wireless-Powered Networks," *IEEE Wireless Communications Letters*, vol. 8, no. 5, pp. 1373–1376, Oct. 2019.

[6] T. Long *et al.*, "Energy Neutral Internet of Drones," *IEEE Communications Magazine*, vol. 56, no. 1, pp. 22–28, Jan. 2018.

[7] M. Mozaffari *et al.*, "A Tutorial on UAVs for Wireless Networks: Applications, Challenges, and Open Problems," *IEEE Communications Surveys Tutorials*, vol. 21, no. 3, pp. 2334–2360, thirdquarter 2019.

[8] ——, "Efficient Deployment of Multiple Unmanned Aerial Vehicles for Optimal Wireless Coverage," *IEEE Communications Letters*, vol. 20, no. 8, pp. 1647–1650, Aug. 2016.

[9] M. Alzenad *et al.*, "3-D Placement of an Unmanned Aerial Vehicle Base Station (UAV-BS) for Energy-Efficient Maximal Coverage," *IEEE Wireless Communications Letters*, vol. 6, no. 4, pp. 434–437, Aug. 2017.

[10] H. He *et al.*, "Joint Altitude and Beamwidth Optimization for UAV-Enabled Multiuser Communications," *IEEE Communications Letters*, vol. 22, no. 2, pp. 344–347, Feb. 2018.

[11] M. Hifi and R. M'Hallah, "A Literature Review on Circle and Sphere Packing Problems: Models and Methodologies," https://www.hindawi.com/journals/aor/2009/150624/abs/, 2009.

[12] C. A. Balanis, *Antenna Theory: Analysis and Design*. John Wiley & Sons, Feb. 2016.

[13] "Federal Communications Commission CFR, Title 47, Volume 1, Part 15," https://www.govinfo.gov/app/details/CFR-2010-title47-vol1, 2010.

[14] O. Cetinkaya and O. B. Akan, "Electric-Field Energy Harvesting From Lighting Elements for Battery-Less Internet of Things," *IEEE Access*, vol. 5, pp. 7423–7434, 2017.

[15] S. T. Sliper *et al.*, "Energy-driven computing," *Philosophical Transactions of the Royal Society A: Mathematical, Physical and Engineering Sciences*, vol. 378, no. 2164, p. 20190158, Feb. 2020.

[16] P. N. Alevizos and A. Bletsas, "Sensitive and Nonlinear Far-Field RF Energy Harvesting in Wireless Communications," *IEEE Transactions on Wireless Communications*, vol. 17, no. 6, pp. 3670–3685, Jun. 2018.

[17] M. Cardei *et al.*, "Maximum network lifetime in wireless sensor networks with adjustable sensing ranges," in *WiMob'2005), IEEE International Conference on Wireless And Mobile Computing, Networking And Communications, 2005.*, vol. 3, Aug. 2005, pp. 438–445 Vol. 3.

[18] B. Liu and D. Towsley, "A study of the coverage of large-scale sensor networks," in *2004 IEEE International Conference on Mobile Ad-Hoc and Sensor Systems (IEEE Cat. No.04EX975)*, Oct. 2004, pp. 475–483.

[19] D. W. Cantrell, "Packing unit circles in circles: New results," https://groups.google.com/d/msg/sci.math/SMr66-MEH9k/PoMJIKhB3KwJ, Dec. 2008.

[20] E. Specht, "The best known packings of equal circles in a circle," http://hydra.nat.uni-magdeburg.de/packing/cci/cci.html#Applications, Aug. 2014.

[21] E. Yanmaz, R. Kuschnig, and C. Bettstetter, "Channel measurements over 802.11a-based UAV-to-ground links," in *2011 IEEE GLOBECOM Workshops (GC Wkshps)*, Dec. 2011, pp. 1280–1284.

[22] D. Balachander, T. R. Rao, and G. Mahesh, "RF propagation investigations in agricultural fields and gardens for wireless sensor communications," in *2013 IEEE Conference on Information Communication Technologies*, Apr. 2013, pp. 755–759.

[23] S. D. Assimonis, S.-N. Daskalakis, and A. Bletsas, "Sensitive and Efficient RF Harvesting Supply for Batteryless Backscatter Sensor Networks," *IEEE Transactions on Microwave Theory and Techniques*, vol. 64, no. 4, pp. 1327–1338, Apr. 2016.

[24] S.-E. Adami *et al.*, "A Flexible 2.45-GHz Power Harvesting Wristband With Net System Output From -24.3 dBm of RF Power," *IEEE Transactions on Microwave Theory and Techniques*, vol. 66, no. 1, pp. 380–395, Jan. 2018.